CHAIN-BRANCHING AND INITIATION RATES MEASURED BY SPATIALLY INTEGRATED LIGHT EMISSION DURING REFLECTED SHOCK-WAVE IGNITION

GARRY L. SCHOTT

University of California, Los Alamos Scientific Laboratory, Los Alamos, New Mexico

Experimental study of ignition kinetics in H_2–O_2–CO–Ar mixtures by time-resolved photoelectric measurement of the growth of spatially integrated CO–O recombination radiation in reflected shock waves has been extended to cover the ranges $0.1 \leq H_2{:}O_2 \leq 10.0$, $1000° \leq T \leq 2500°K$, by confining the reactive gas to the downstream end of the shock tube and increasing sensitivity through a large solid angle optical view. The induction period regime of exponential growth of emission intensity, $I(t) \approx I_0^* \exp(\alpha^* t)$, yields precise values of α^* whose dependence upon $[H_2]$, $[O_2]$, and T determines, for the reactions

$$H + O_2 \xrightarrow{k_1} OH + O$$

$$O + H_2 \xrightarrow{k_2} OH + H$$

$$OH + H_2 \xrightarrow{k_3} H_2O + H,$$

the functions: $k_1 = 8.6 \times 10^8 \exp\{-(12.3 \pm 1)$ kcal/mole $(1/T - 1/1600)/R\}$ liter/mole/sec and $k_2k_3 = 1.5 \times 10^{19} \exp\{-(20 \pm 4)$ kcal/mole $(1/T - 1/1600)/R\}$ liter^2/mole^2/sec^2, and indicates that k_2 and k_3 are, at most, about a factor of 3 from each other, in the present temperature range. The early growth of $I(t)$ prior to the exponential regime, now observed directly, and the parameter I_0^*, now fairly precisely measured, bear upon the kinetics of chain initiation but require further investigation.

Introduction

Since the discovery and time-resolved measurement of intense ultraviolet emission during the branching chain phase of shock-wave initiated acetylene–oxygen combustion,[1] there have been several similar measurements of exponential growth of electronic emission[2–4] from such molecules as CH, CO, and OH, and of ionization,[5] occurring as side reactions in presumably fixed but *a priori* unknown relationship to the progress of the main chemical chain. Using first mass spectrometry[6] and, more recently, infrared emission,[7] Kistiakowsky and co-workers have recorded exponentially growing formation of primary chain-reaction products in hydrocarbon combustion in shock waves. Also recently, Gutman and Schott (specified hereinafter as G-S)[8] studied the growth of CO–O (blue "continuum") recombination radiation in shock-wave ignited H_2–O_2–CO–Ar mixtures, in order to determine the chain-branching rate from the increase in O atom population in the presence of an excess of CO Direct determination of the chain-branching kinetics in combustion reactions, apart from the initiation rate, is one step in unraveling the kinetics of the whole induction-period behavior.

The former studies of emission[1–7] have used collimation through slits at the side of the shock tube to resolve the induction zone near the shock front and exclude interfering light from the highly luminous region of gross combustion somewhat farther upstream. The intensity of the CO–O recombination radiation, when limited by the source volume and solid angle afforded by such slits, was found to be insufficient for precise measurement for growth constants in the 10^{-5} sec range, and the technique of spatially integrated viewing of reflected shock waves was introduced.[8] This technique depends upon the principle that so long as the luminosity everywhere between the end plate and the reflected shock front is growing with a given exponential rate, the spatially integrated intensity reaching a detector also

grows with that exponential rate, even though the time origin and the solid angle of view each depend upon position.

The initial study[8] was restricted to low temperatures and/or densities by the equipment used, and was confined to H_2:O_2 ratios of 1 or greater to afford primary sensitivity to the rate of Reaction (I) of the chain-reaction sequence

$$H + O_2 \xrightarrow{k_1} OH + O, \qquad (I)$$

$$O + H_2 \xrightarrow{k_2} OH + H, \qquad (II)$$

$$OH + H_2 \xrightarrow{k_3} H_2O + H, \qquad (III)$$

$$H + O_2 + M \xrightarrow{k_4} HO_2 + M. \qquad (IV)$$

Subsequent work by Gutman and co-workers has dealt with the effect of the chain-breaking Reaction (IV) (hereinafter referred to as GHDL),[9] and with the relationship between the growth rates of the OH $^2\Sigma^+ \rightarrow {}^2\Pi$ and CO–O emissions.[10] The present paper reports further experimental work with the spatially integrated CO–O emission technique in reflected shock waves, extending the measurements on H_2–O_2–CO–Ar mixtures to higher temperatures and an order-of-magnitude faster exponential growth rates than measured previously, and concentrating on definition of the dependence of the H_2–O_2 chain branching rate upon the H_2 concentration through the rates of Reactions (II) and (III). With the larger initiation rates obtained at the higher temperatures, and with the larger sensitivity described below, direct exploration of the initiation phase of the reaction has also been realized, although the results obtained so far do not appear to be altogether satisfactory.

Experimental

The main extensions in the experimental technique introduced in the present work are indicated in the schematic diagram of the downstream end of the shock tube shown in Fig. 1.

First, a matching-bore rotating plug valve was placed in the 10-cm-i.d. shock tube so that only a 60-cm Pyrex-walled test section at the downstream end was filled with the combustible H_2–O_2–CO–Ar mixture. The valve body and the buffer section upstream contained an exactly equal pressure of Ar or a mixture of Ar, N_2, and H_2 having the same molecular weight and sound speed as the test gas, to prevent layering when the valve was opened and to transmit the unreactive incident shock wave completely. Ignition in the incident wave, if it required more than ca. 600 μsec, was thus delayed until after reflection had occurred at the end plate.

Second, in an attempt to provide greater precision in incident shock-velocity measurement than had been achieved with our previous electronic techniques employing 2-mm-diam piezoelectric gauges mounted in the walls, a system of five shadow-light screens was used. This system employed a He–Ne gas laser source and adjustable beam splitters to provide accurately parallel beams projecting events in the shock tube onto external knife edges spaced 10.00 cm apart in an Invar plate. The refraction shadow of the thin shock front is broadened by Fresnel diffraction, and electronic resolution of the resulting beam perturbation, together with nonideal attenuation[11] of the shock waves, prevented determination of the shock speed at the end plate to within better than a few tenths of 1%.

The telecentric optical system employed by G-S afforded much greater sensitivity than a side-slit system because of the larger volume viewed, and at the same time provided a spatially homogeneous view. To measure CO–O emission growing exponentially with time constants between 0.5 and 2×10^6 sec^{-1} under the density and temperature conditions of the present experiments, it was found necessary to use large solid angles as well, and the end-window photomultiplier (10 stage, S-11 response, 1.5-in.-diam cathode, RCA type 2020), wired for linear response to large pulses and gain near 1×10^4, was placed adjacent to the transparent end plate as shown in Fig. 1. With this arrangement, the time resolved,

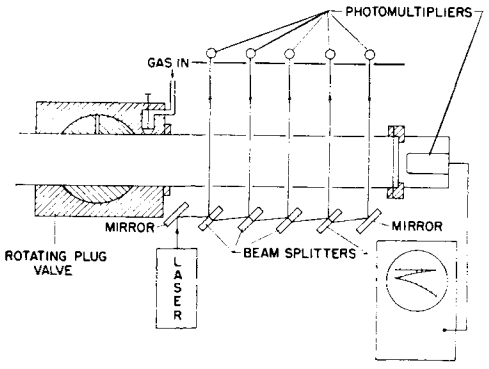

FIG. 1. Schematic diagram of test section for spatially integrated emission measurements in reflected shock waves.

spatially integrated intensity $I(t)$ can be formulated as

$$I(t) = \int_0^{v_{rs}t} \int_0^{r_0} 2\pi r D(x, r) f_{CO} \times \sum_{i=0}^{3} B_i \exp\{\alpha_i[t - (x/v_{rs})]\}\, dr\, dx, \quad (1)$$

where t is measured from the instant of shock-wave reflection, x is measured axially upstream from the end plate to the reflected shock front at $v_{rs}t$, and r is measured from the tube axis to the wall at r_0. D is the geometric and instrumental detectivity function for emitted light, and f_{CO} is the emission intensity factor per unit concentration of oxygen atoms. These factors depend upon position and constant properties of the shock wave, but not upon time. The summation represents the growing oxygen-atom concentration during the induction period [see Eq. (3) below]. α_0 is zero and only α_1 is positive, so that ultimately $I(t)$ is dominated by the term

$$I_0 \exp(\alpha_1 t) = (v_{rs}/\alpha_1) \exp(\alpha_1 t) \times \int_0^{v_{rs}t} \int_0^{r_0} 2\pi r D(x, r) f_{CO} B_1 \times \exp(-\alpha_1 x/v_{rs})\, dr\, (\alpha_1/v_{rs}) dx, \quad (2)$$

wherein the integral approaches a constant as t becomes large.

Finally, a multiple-trace (zigzag raster) oscilloscope presentation was employed to improve the precision of time determination during the rapid exponential increase of the emission signal by providing faster sweeps without requiring correspondingly more-precise synchronization. An example of the multiple-trace records is presented in Fig. 2, where the freedom of the signal from noise and the superimposed half-microsecond timing marks are evident. Actually, the amplitude range of this presentation is less than that of a single sweep, because the smallest signals are obscured by the overwritten earlier trace(s). In many of the experiments, a second oscilloscope, set for higher gain and single sweep, was used to record the early course of the emission. Frequently, this earlier record showed the initiation transient, and not the desired exponential growth. In addition, an auxiliary timing trace was recorded which related the timing-marker sequence of the amplitude presentations to the arrival of the shock wave at the end window, detected by an evaporated metal resistance gauge on its inside surface.

Standard gas-handling techniques were used, and blank experiments similar to those described by G-S were done with the present setup.

Results

Table I presents the manometrically measured compositions of the gas mixtures studied, the unshocked gas pressures p_0, and the numbers of experiments performed in each set. Figure 3 shows an example of a semilogarithmic plot of CO–O emission intensity against time, illustrating: (i) the range covered by the zigzag oscilloscope record; (ii) the early nonexponential growth recorded by the higher gain, single-sweep

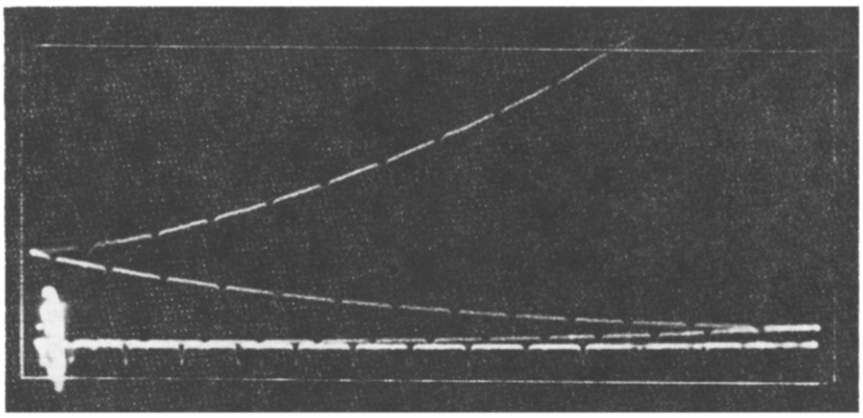

FIG. 2. Multiple-trace oscillogram of emission growth and 0.50-μsec timing marks in sample experiment in Mixture IIB (see Table I); p_0 = 100 Torr, reflected shock temperature = 2168°K, α^* = 2.52 × 10^5 sec^{-1}.

TABLE I

Resume of initial conditions of experiments

Mixture	Mixture composition, %					Numbers of experiments	
	H_2	O_2	CO	CO_2	Ar	p_0 = 50 Torr	p_0 = 100 Torr
I	2.25	0.75	1.99	—	95.01	7	6
IA	2.22	0.74	1.97	0.99	94.08	—	4
II	0.76	2.28	2.07	—	94.89	4	6
IIA	0.76	2.28	4.04	—	92.92	5	16
IIB	0.25	0.76	2.03	—	96.96	6	10
III	0.73	6.94	3.86	—	88.47	9	—

oscilloscope; (iii) the straight line determined by the exponentially growing component of the signal, whose slope is the primary observable quantity which we denote α^*; and (iv) the extrapolation of this line to the time of shock-wave reflection, which determines the intercept I_0^*, the measured coefficient of the exponentially growing component of the emission.

The values of α^* from the 73 experiments covering the reflected-shock temperature range 1500°–2500°K for H_2:O_2 = 3.0 (Mixtures I) and H_2:O_2 = 0.33 (Mixtures II), and the lower part of this range for H_2:O_2 = 0.1 (Mixture III), are correlated by division by twice the prevailing O_2 concentration, and the resulting function is plotted semilogarithmically against reciprocal temperature in Fig. 4. This plot separates the data into groups according to the H_2:O_2 ratio. It demonstrates the essential proportionality of α^* to the density of reactants, i.e., to $[H_2]$ or to $[O_2]$, for Mixtures I, II, IIA, and IIB, and it suggests the relationship of α^* to its presumed upper bound, $2k_1[O_2]$. Also indicated in this plot are the observed failure of addition of 1% CO_2 to Mixture I to affect α^*, and the failure of [CO] to affect α^*, as a result of which the data from Mixtures II and IIA were found to form single groups of points whose scatter is comparable to that of any of the other groups. Three of the experiments with Mixture IIA differed from the others in that the test gas from the reservoir was admitted into the downstream end of the shock tube through a dry-ice cooled U-tube trap just outside the sample inlet valve shown in Fig. 1. The points in Fig. 4 show that this procedure likewise did not change the measured α^* from that found under the same conditions without the trapping. One can also observe by comparing Fig. 4 with the corresponding plots in earlier papers[8,9] that the scatter in the measurement of α^* as a function of temperature has been improved by the combination of techniques used in the present work.

The values of I_0^* were measured in the experiments with Mixtures I, II, and IIA under uniform instrumental conditions. While the scatter was considerable (±20% rms, estimated), in each mixture I_0^* was found to increase sharply with temperature and to be independent of reactant density. Moreover, the I_0^*-vs-temperature curves for Mixtures II and IIA were indistinguishable. Matching experiments in Mixtures I and IA yielded the same values of I_0^*, showing no effect of the added CO_2, and the admission of

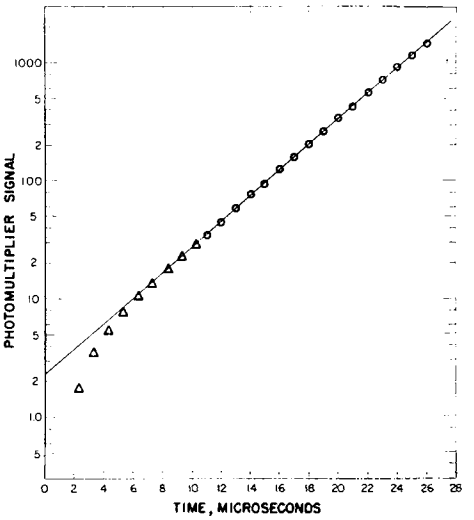

FIG. 3. Semilogarithmic plot of spatially integrated CO–O emission against time for experiment shown in Fig. 2. ○, data from zigzag oscillogram; △, data from high-sensitivity, single-trace oscillogram.

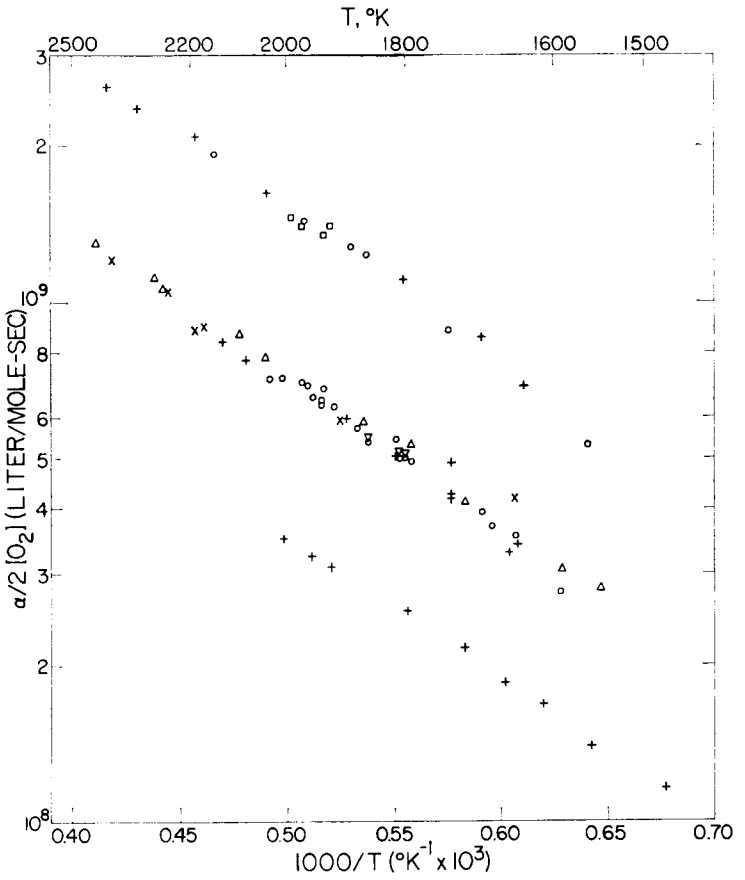

FIG. 4. Plot of temperature dependence of measured exponential growth-coefficient data, $\alpha^*/2[O_2]$, for experiments in gas mixtures given in Table I. + and ×, p_0 = 50 Torr; open symbols, p_0 = 100 Torr. Upper group: + and ○, Mixture I; □, Mixture IA. Middle group: + and ○, Mixtures II and IIA; ▽, Mixture IIA admitted through trap; × and △, Mixture IIB. Lower group: +, Mixture III.

Mixture IIA through the trap also did not change I_0^*.

Interpretation

Kinetic Equations

The growth of oxygen-atom concentration during the induction period of the reaction occurring in the present H_2–O_2–CO–Ar mixtures, and under the conditions of the reflected shock-wave experiments, is supposed to be determined adequately by the rates of Reactions (I)–(IV), proceeding irreversibly in a medium of fixed temperature and H_2, O_2, and total gas concentrations, and accompanied by unspecified reactions producing H, O, and/or OH at the constant rates R_1, R_2, and R_3, respectively. The product H_2O, the CO, and the HO_2 formed are regarded as inert on the supposition that the reactions of these molecules are too slow to affect the course of the rapid ignition materially. From the set of linear rate equations for [H], [O], and [OH], the [O] profile after time t_0 is given by

$$[O](t) = \sum_{i=1}^{3} B_i \exp[\alpha_i(t - t_0)] + B_0, \quad (3)$$

where the exponential coefficients α_i are the three roots of the auxiliary equation

$$\alpha^3 + (K_1 + K_2 + K_3 + K_4)\alpha^2 + [K_2K_3 + (K_2 + K_3)K_4]\alpha - K_2K_3(2K_1 - K_4) = 0, \quad (4)$$

in which $K_1 = k_1[O_2]$, $K_2 = k_2[H_2]$, $K_3 = k_3[H_2]$, and $K_4 = k_4[O_2][M]$. The B_i are constant coefficients whose sum, including the term

$$B_0 = -[K_1(R_1 + R_3) + K_4R_2]/K_2(2K_1 - K_4),$$

which arises from the particular solution of the inhomogeneous equations, is equal to the value of $[O]$ at $t = t_0$.

So long as $(2K_1 - K_4)$ is positive (a condition already presumed in neglecting HO_2 decomposition), uninhibited branched-chain explosion occurs. One and only one of the roots, α_1, is positive, and the other two are either negative or are complex conjugates with negative real part. In the latter case, the shorthand form given in Eq. (3) is deceptively simple. Because the term $B_1 \exp(\alpha_1 t)$ ultimately dominates $[O](t)$, the important coefficient is B_1, which of course must be positive. B_1 is determined by the value of $[O]$ at t_0 in conjunction with its relationship to the corresponding coefficients of the terms in

$$[H](t_0) = \sum_{i=0}^{3} A_i$$

and

$$[OH](t_0) = \sum_{i=0}^{3} C_i.$$

The important ratios are

$$B_1/A_1 = K_1/(\alpha_1 + K_2)$$

and

$$B_1/C_1 = K_1K_3/\{\alpha_1^2 + (K_1 + K_2 + K_4)\alpha_1 + K_2K_4\}.$$

Ideally, t_0 is taken immediately behind the reflected shock wave and the initial radical concentrations are zero, but the possibility of initiation by a burst of radicals from an impurity reacting "instantaneously" or in the incident shock is handleable by nonzero initial values at t_0. B_1 is thus sensitive to the whole set of particular solutions involving the R's, and to any initial value term that may be large enough to have influence.

α^* Data

To interpret the measured emission growth coefficients α^*, we are interested in the positive root of Eq. (4), α_1, and its dependence upon the experimental variables $[H_2]$, $[O_2]$, $[M]$, and T conveyed through the K's. Insofar as the influence of Reaction (IV) is minor and may be allowed for by using an independently determined value of k_4 for an argon environment, the data on α^* at three H_2:O_2 ratios over a common temperature range provide three independent conditions on the coefficients k_1, k_2, and k_3. However, because k_2 and k_3 enter Eq. (4) interchangeably through the sum and product of K_2 and K_3, only $(k_2 + k_3) \equiv k_s$ and $k_2k_3 \equiv k_p$ may be determined unambiguously. Also, trial hand calculations with graphically smoothed data revealed the possibility of complex conjugate values being obtained for k_2 and k_3 by literal deduction from slightly inaccurate data, through the indicated value of k_s being smaller than $2(k_p^{1/2})$, which is its minimum value for real k's. For these reasons, subsequent analysis was pursued in terms of k_s and k_p directly.

Data from the 73 experiments in Fig. 4 were treated by a computer program for the Gauss iterative approach to the nonlinear least-squares problem,[13] by which $\sum(\alpha^* - \alpha_1)^2$ was minimized with respect to variation of Arrhenius parameters representing the temperature-dependent coefficients k_1, k_p, and k_s, using fixed parameters from GHDL for k_4. The formulations used for the adjustable k's were: $k_1 = A_1 \exp(-E_1/RT)$; $k_p = A_p \exp(-E_p/RT)$, in which A_p represents A_2A_3, and E_p represents $(E_2 + E_3)$; and either $k_s = A_s \exp(-E_s/RT)$ or $k_s = 2(k_p^{1/2})$, both of which are somewhat artificial. Analysis with the first form of k_s yielded estimates of the parameters and their standard deviations indicating that k_1 was determined most precisely ($1.85 \pm 0.05 \times 10^9$ liter/mole/sec at 2000°K, $E_1 = 11.9 \pm 0.7$ kcal/mole), k_p was determined next best ($53 \pm 4 \times 10^{18}$ liter^2/mole^2/sec^2 at 2000°K, $E_p = 19.1 \pm 2.3$ kcal/mole), and k_s was least well established ($8.4 \pm 2.0 \times 10^9$ liter/mole/sec at 2000°K, $E_s = -2 \pm 5$ kcal/mole). This estimate of k_s is clearly smaller than the admissible minimum, $2(k_p^{1/2})$, but not by a large factor, and becomes relatively larger at lower temperatures. As k_s is not sensitively determined by the data, it was concluded provisionally that k_2 and k_3 are approximately equal in the temperature range of the experiments. The second formulation of k_s embodies this conclusion, and its use yielded substantially as good a fit to the data [$\sum(\alpha^* - \alpha_1)^2$ was increased 12%], with four adjustable parameters instead of six. The values of k_1 and k_p were not materially affected, although both activation energy parameters were increased (to $E_1 = 12.8$ and $E_p = 24.5$ kcal/mole) in compensating for the constrained temperature dependence of k_s.

In an attempt to refine the parameters given above for k_1 and k_p, particularly the activation

energies that are based on a small range of $1/T$ and are not quite consistent with literature data obtained below 1000°K, and also to examine the consistency of the present data with those obtained with the earlier[8,9] setup in lower ranges of α^* and temperature, the present data were merged with the $H_2:O_2 = 10.0$ and the $H_2:O_2 = 3.0$, $T \geq 1190$°K data from G-S and the $H_2:O_2 = 1.0$, $[M] \leq 2.5 \times 10^{-2}$ mole/liter and the $H_2:O_2 = 0.33$, $[M] \leq 0.9 \times 10^{-2}$ mole/liter data from GHDL. The resulting parameter estimates were: for Arrhenius k_s,

$$k_1(1600°K) = 0.856 \times 10^9 \text{ liter/mole/sec},$$

$$E_1 = 12.3 \text{ kcal/mole},$$

$$k_p(1600°K) = 15.0 \times 10^{18} \text{ liter}^2/\text{mole}^2/\text{sec}^2,$$

$$E_p = 20.0 \text{ kcal/mole},$$

$$k_s(1600°K) = (7.6 \pm 1.4) \times 10^9 \text{ liter/mole/sec},$$

and

$$E_s = 1.1 \pm 3.0 \text{ kcal/mole};$$

for

$$k_s = 2(k_p^{1/2}),$$

$$k_1(1600°K) = 0.864 \times 10^9,$$

$$E_1 = 13.3,$$

$$k_p(1600°K) = 15.5 \times 10^{18},$$

and

$$E_p = 23.7.$$

The discrepancies between the two sets of parameters for k_1 and k_p are regarded as fairer estimates of their uncertainties than are the very small statistically calculated standard deviations.

The sensitivity of k_1 and k_p to the data, and the relative insensitivity of k_s, can be interpreted on the basis that the limiting values of α_1 from Eq. (4) at very large and very small $H_2:O_2$ ratios are $(2K_1 - K_4)$ and

$$(2K_p)^{1/2}[(K_1 - K_4/2)/(K_1 + K_4)]^{1/2} \approx (2K_p)^{1/2},$$

respectively. Thus, the mixtures with $H_2:O_2$ ratios of 3.0 and 0.1 afford sensitivity to these two quantities primarily. The situation in the middle of the range of our data is illustrated by the following values of partial derivatives evaluated from Eq. (4) using the parameters determined by least squares, for conditions

$$H_2:O_2 = 0.33,$$

$$T = 2009°K;$$

$$\partial \ln \alpha_1/\partial \ln k_1 = 0.49;$$

$$\partial \ln \alpha_1/\partial \ln k_p = 0.34;$$

$$\partial \ln \alpha_1/\partial \ln k_s = -0.16;$$

and

$$\partial \ln \alpha_1/\partial \ln k_4 = -0.03.$$

The present result that k_2 and k_3 are nearly equal near 2000°K requires re-examination of the approximate procedure used by G-S to extract values of k_1 and k_2 from pairs of α^* and $H_2:O_2$ ratio data, which was derived by supposing k_3 to be large enough to be cancelled from Eq. (4). The statement by G-S that values of the k's obtained by this procedure agree to three significant figures with values derived substituting a literature value of k_3 into Eq. (4) has been traced to a numerical error. Consideration of the terms neglected in the G-S procedure, or the physical argument that that procedure blames all of the observed dependence of α_1 upon $[H_2]$ on the smallness of k_2, leads to the conclusion that the G-S estimate of k_2 is in fact a lower bound to k_2, or equivalently to k_3 because of the symmetry of k_2 and k_3 in Eq. (4).

Examination of the present results in terms of such a lower bound shows that the $H_2:O_2 = 0.1$ or 0.33 data, together with k_1, determine a lower value of this bound than the G-S value, which was based on data at $H_2:O_2 \geq 1.0$. The greatest and most-precise lower bound to k_2 (and k_3) from the available data is found empirically to be obtained by combining the $H_2:O_2 = 1.0$ data from G-S and GHDL with the value of k_1 determined above and an artificially very large value of k_3 in the least-squares treatment. The result is k_2 (or k_3) $\geq (2.16 \pm 0.7) \times 10^9 \exp[-(14.8 \pm 0.7)$ kcal/mole $(1/T - 1/1600)/R]$ liter/mole/sec, which is comparable to the G-S result. Acceptance of the least-squares value of k_p, and its uncertainties, and dividing it by the lower bound, determines the upper bound: k_3 (or k_2) $\leq (7.0 \pm 1) \times 10^9 \exp[-(5.2 \pm 5)$ kcal/mole $(1/T - 1/1600)/R]$ liter/mole/sec over the 1000°–2000°K range of the $H_2:O_2 = 1.0$ data. These bounds indicate that $0.3 \lesssim k_2/k_3 \lesssim 3.2$ near 1600°K, with wider bounds at lower temperatures, confirming the less-specific conclusion reached from the k_s and k_p results.

In conclusion, then, the model represented by Eqs. (2)–(4) suffices to describe the measurements of α^* over the ranges $0.1 \leq H_2{:}O_2 \leq 10.0$, $1000° \leq T \leq 2500°K$, $[M] \leq 0.05$ mole/liter, if one accepts the insensitively determined anomaly $k_s < 2(k_p^{1/2})$ above about 1500°K. The results determine the rate coefficient functions:

$$k_1 = 8.6 \times 10^8 \exp\{-(12.3 \pm 1) \text{ kcal/mole} \times (1/T - 1/1600)/R\} \text{ liter/mole/sec}$$

and

$$k_2k_3 = 1.5 \times 10^{19} \exp\{-(20 \pm 4) \text{ kcal/mole} \times (1/T - 1/1600)/R\} \text{ liter}^2/\text{mole}^2/\text{sec}^2,$$

with the behavior of k_s and the lower bound to k_2 and k_3 indicating that $k_2 \approx k_3$ above 1500°K.

I_0^* Data

From Eq. (2) we see that I_0 is proportional to B_1 and to f_{CO}, the emission intensity factor per unit oxygen-atom concentration; it is inversely proportional to α_1, and is otherwise determined by substantially constant factors. α_1, as measured by α^*, has been found to be proportional to reactant (i.e., H_2 or O_2) concentrations and independent of [CO]. The observation that I_0^* is independent of mixture density and independent of exchanging CO for Ar then indicates that the product $f_{CO}B_1$ is proportional to density and independent of [CO]. On the hypothesis that initiation of the chain oxidation reaction occurs by slow reactions, producing reactive species at the constant rates R_j, and not by impurities, B_1 is proportional to a linear combination of the R_j whose coefficients are inversely proportional to density. For irreversible, elementary initiation reactions of total order n, B_1 is then proportional to density to the power $(n-1)$. If $n = 2$, as one would expect, then the lack of dependence of I_0^* upon both density and [CO] indicates that f_{CO} is independent of [CO]. However, the initial hypothesis[8] by which f_{CO} was presumed to be independent of time during the induction period implicitly supposed that it was proportional to [CO]. Moreover, this anomaly is not removed by supposing B_1 to have some other dependence upon density, as might be the case if initiation were impurity controlled, unless B_1 is also somehow inversely proportional to [CO]. Further study is needed to resolve this matter before the I_0^* data from experiments of the present type can be used directly to draw conclusions about chain-reaction initiation.

Acknowledgments

This work was performed under the auspices of the United States Atomic Energy Commission. The assistance of J. L. Young and J. G. Williamson in the experimental work, and key consultations with Professor David Gutman and Professor John H. Kiefer are gratefully acknowledged.

References

1. Kistiakowsky, G. B. and Richards, L. W.: J. Chem. Phys. *36*, 1707 (1962).
2. Gardiner, Jr., W. C., Mallard, W. G., Morinaga, K., Ripley, D. L., and Walker, B. F.: *Eleventh Symposium (International) on Combustion*, p. 1151, The Combustion Institute, 1967, and references cited therein.
3. Gay, I. D., Glass, G. P., Kern, R. D., and Kistiakowsky, G. B.: J. Chem. Phys. *47*, 313 (1967), and references cited therein; Homer, J. B. and Kistiakowsky, G. B.: *ibid.* *45*, 1359 (1966).
4. Belles, F. E. and Lauver, M. R.: J. Chem. Phys. *40*, 415 (1964).
5. Hand, C. W. and Kistiakowsky, G. B.: J. Chem. Phys. *37*, 1239 (1962), and subsequent work cited in Refs. 2 and 3 above.
6. Glass, G. P., Kistiakowsky, G. B., Michael, J. V., and Niki, H.: *Tenth Symposium (International) on Combustion*, p. 513, The Combustion Institute, 1965; J. Chem. Phys. *42*, 608 (1965).
7. Homer, J. B. and Kistiakowsky, G. B.: J. Chem. Phys. *47*, 5290 (1967); *ibid.* *46*, 4213 (1967).
8. Gutman, D. and Schott, G. L.: J. Chem. Phys. *46*, 4576 (1967).
9. Gutman, D., Hardwidge, E. A., Dougherty, F. A., and Lutz, R. W.: J. Chem. Phys. *47*, 4400 (1967).
10. Gutman, D., Lutz, R. W., Jacobs, N., Hardwidge, E. A., and Schott, G. L.: J. Chem. Phys. *48*, 5689 (1968).
11. Emrich, R. J. and Curtis, C. W.: J. Appl. Phys. *24*, 360 (1953).
12. Kondratiev, V. N.: Chemical Kinetics of Gas Reactions, p. 518, Academy of Sciences, U.S.S.R., Moscow, 1958; English transl.: p. 614, Pergamon Press, 1964.
13. Moore, R. H. and Zeigler, R. K.: The Solution of the General Least Squares Problem with Special Reference to High-Speed Computers, Los Alamos Scientific Laboratory Report LA-2367, 1960.

COMMENTS

A. G. Gaydon, Imperial College, London. The character of the CO flame spectrum depends upon temperature; in hot flames, the ultraviolet region is relatively much stronger. Thus, the emission intensity will depend upon the temperature as well as upon the CO–O reaction rate, and the result may also appear to depend upon the wavelength at which the measurements are made. Does this introduce any correction?

G. L. Schott. The dependence of the CO flame spectrum upon temperature should have no effect upon the measurement of the exponential growth coefficients because, apart from possible boundary-layer cooling at the window, each experiment is isothermal during the induction period when the exponential growth occurs. To be sure, the spectral distribution and/or the spectrally integrated intensity of the emission are expected to contribute to the temperature dependence of the amplitude factor, I_0*. However, the seemingly anomalous behavior of I_0* is revealed by comparisons at a common temperature and an unchanged spectral response of the photodetection equipment.

Supporting evidence that the CO flame-spectrum intensity does reveal essentially the correct exponential time constant of the branching chemical chain in the present system is offered by the first results of measurements of the growth of infrared emission intensity near 2.7 microns (H_2O and some OH, possibly) in the ignition of H_2–O_2–Ar mixtures without added CO. This work is being pursued by my colleagues R. W. Getzinger, L. S. Blair, and D. B. Olson.

F. Kaufman, University of Pittsburgh. It should be pointed out that the activation energy obtained in this work for the reaction $H + O_2 \rightarrow OH + O$ is about 4 kcal/mole lower than the endothermic heat of reaction. The latter is fairly insensitive to reaction temperature. Is this discrepancy resolvable within the probable errors of the present investigation?

G. L. Schott. Professor Kaufman has drawn attention to the particularly conspicuous anomaly in the temperature dependence of the values of k_1 derived from the data, whereby the activation energy parameter, $E_1 = 12.3 \pm 1.0$ kcal/mole, is found to be smaller than the thermochemical ΔE for the reaction. As the text of the paper notes without elaboration, this value of E_1 is also noticeably smaller than the E_1 that relates lower temperature determinations of k_1 to each other or to any representative value from the present investigation. Moreover, the parameter $E_p = (E_2 + E_3) = 20 \pm 4$ kcal/mole is also found to be anomalous, not in relation to thermochemistry, but in comparison to the low-temperature evidence pertaining to E_2 and E_3 separately, by which E_p should not exceed about 15 kcal/mole.

From consideration of the graphical representation of the α* data (Fig. 4), and of the variations in the statistical treatment performed, I do not believe that these anomalies are reconcilable within the scatter of the data, or within the ambiguity of the representation of k_s. Of course, it is possible that these activation-energy anomalies and the anomalies simultaneously observed in I_0* and k_s do indicate some systematic inadequacy in the experimental data or in the kinetic treatment used to interpret them. Likely causes of experimental error, all of which are expected to be more serious at higher temperatures, might be: (a) cooling of the gas adjacent to the end wall; (b) vanishing of the truly exponential character of the ignition as initiation transients persist, until they merge with depletion effects; and (c) failure of the CO flame-spectrum intensity, or the instrumental recording thereof, to follow faithfully the more-rapid chain-branching progress. If one chooses to associate the above anomalies with probable errors, then the answer to Kaufman's question is affirmative, with the qualification that the errors are systematic. However, I do not find the evidence conclusive as to the magnitude of such errors, and the paper as a whole emphasizes the new elements of experimental technique and, secondarily, the range of conditions and sensitivity to experimental variables embraced by its application, with the elementary chemical kinetics results relegated to third position and represented by empirical equations constrained to have simple Arrhenius form.

In considering anomalies in activation energies arising from measurements made at the temperatures of combustion processes, and their seriousness in relationship to orthodox chemical kinetics concepts, we might observe two factors. First, the accessible range of $1/T$, and thus the range of the magnitude of a rate coefficient k, is typically much smaller at combustion temperatures than it is near room temperature. Thus, a deficit of 4 kcal/mole, which would correspond to more than a factor of 100 error over a 900°K

range from 300° to 1200°K, is logarithmically less than one-tenth as serious over the 1600°–2500°K range, and could arise from data correct at 1600°, but systematically diminishing to 63% of the correct value at 2500°K. This temperature range is equivalent, in $1/T$, only to that between 27° and 49°C. Second, our ideas about the constancy of activation energies, and even about their being bounded from below by the reaction endothermicity, have developed from experience at low temperatures and, I believe, have not really been tested with precision better than about RT. In the present (combustion) regime, RT is from 3 to 5 kcal/mole.